Calibrating Jason-3 against Jason-2

Bachelor's Thesis

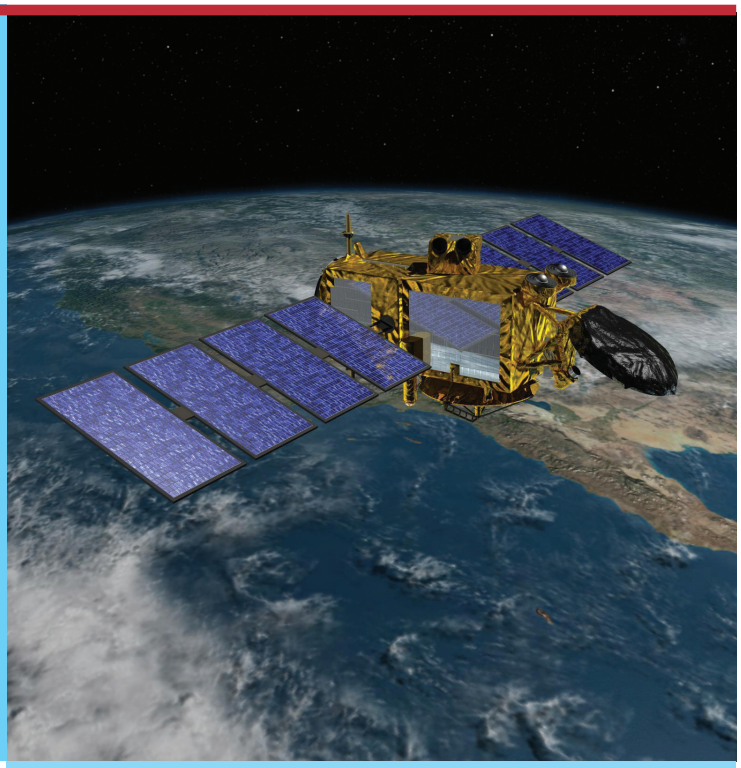

Ida Alberte Egdalen
June 2016

DTU Space
National Space Institute

Denmarks Technical University

Bachelor Project

Jason-3 calibrated against Jason-2

Author:
Ida Alberte Egdalen

Supervisors:
Ole Baltazar Andersen
Karina Nielsen

June 17, 2016

ECTS: 15 points

Abstract

Precise water altimetry applications for sea level monitoring and ocean circulation studies are highly demanded by scientist across the world, for better weather forecasting and improvement of prediction models. Satellite missions to provide this data with highest possible accuracy, is prioritized by international space agencies with Jason-1, Jason-2 and Jason-3 launched January 2016, being one of the most prominent efforts in this respect. In addition to the constant improvement of radial orbit error determination, calibration of both the altimeter as well as investigation of linear trends in the set of geophysical- and range corrections are very important. This report introduces the principle of altimetry as well as the necessary corrections including their typical values. For calibration of Jason-3 against Jason-2, various, although limited data are investigated, including altimetry observations performed across a fixed ground track path of an in-land lake in Sweden, Vänern, in addition with in-situ water station observations. This comparison is followed by analysis of available altimeter crossovers, both single- and dual satellite. The Jason-3 calibration against Jason-2, is based on observations from direct measurements and from crossover results and the associated statistical parameters analyzed. The results are highlighted and discussed including indications of possible future enhanced analysis, with a final conclusion addressing the main findings.

The results of direct comparison of mean values determined at the calibration site, Vänern, show an off-set of 2-3 cm between Jason-2 and Jason-3, where Jason-3 measures the lowest water level height. More significantly, however, is the 30-33 cm difference between the water station and the water level heights observed by the two satellites, suggested to be powered by biases in the media corrections over-estimating the range. Interpretation of the single and dual crossover profiles (difference in sea level anomaly) indicate a lower mean ($\sim$ 0 cm) near Equator and higher variations in difference ranging within 0.5-0.15 cm toward the poles. Overall standard deviations of 5-6 cm is observed for both single- and dual crossovers.

Contents

Introduction

In step with the demands and expectations to today's technology and science development, the space industry deal with the challenge of always being a step ahead in its ability to supply the necessary data to meet the demands. Many years of preparations and technology developments, are invested in a space mission. The Jason-3 satellite mission is no exception. Jason-3 was launched in January 2016 to take over for its predecessor, the Jason-2. The properties for the two sister satellites, and their on-board equipment, are generally the same, however Jason-3 is expected to perform better in terms of data collection of ocean surface heights near coastal lines.

The objective of this report is to calibrate Jason-3 against Jason-2, to maintain Earth water surveillance by Jason-3 of similar character as by Jason-2, while orbiting in the exact same ground tracks. The calibration is performed based on suitable sets of altimetry data for each of the two satellites and comparison with in-situ water station measurements applicable for the Swedish inland lake of Vänern as well as comparing sets of single - and dual crossover results. To attempt to perform as sensible calibration of the two sister satellite measurements, many factors must be considered, evaluated and adjusted. This is rooted in the constant improvements of the quality of the sea surface height observations from satellite altimetry, which of course similarly require constant improvements of associated data corrections. In section 1, the technique behind radar altimetry will be described followed by brief introductions of the individual corrections applied to the orbital altitude in order to derive a sea mean surface height across Vänern. Sections 2 and 3, will introduce the primary data used for calibration and briefly inform on the processing of this data, in order to verify the calibration. Section 4, presents the results and calibration of the Jason-2 results against the Jason-2 results, as derived from the data considered and processed, followed by a thorough examination and discussion of the results in section 5. Finally, section 6 will summarize the various solutions combined with highlights of the main findings.

1 Theory

The Jason-3 Earth observation satellite launched on January 17, 2016, is equipped with various highly accuracy instruments measuring and providing information about water surface heights, tides, currents and modeling, supporting advanced water surface topography, forecasting and evaluation models (NOAA et al., 2015). The primary instrument on-board is the radar altimeter, specifically the Poseidon-3B, capable of reliably mapping the sea surface topography. In this section the general principles of radar altimetry will be elaborated upon as well as a brief clarification of the necessary measurement corrections caused by various interference's of the radar pulse. The principles and theory addressed in this section, are mainly introduced for general reference and not treated or described in any detail, as the focus of this reporting will be on subsequent sections containing the data acquisition and data interpretation.

1.1 Radar altimetry

Radar altimetry is a method used to measure sea surface height from the altimeter range measurement. The technique is fairly simple as follows; the time it takes a radar pulse to make a satellite-to-Earth surface-to-satellite round trip can be calculated into a distance, or range. Conceptually it works by transmitting a pulse of electromagnetic wave radiation towards the Earth's surface, where it is then reflected by the surface and part of the signal is returned to the radar receiver of the altimeter. The estimated round-trip time of the wave is proportional to the satellites altitude. The observed surface height is then the difference between the satellite's position in orbit with respect to an arbitrary surface, the reference ellipsoid, and the satellite-to-Earth surface range (Rosmorduc et al., 2011).

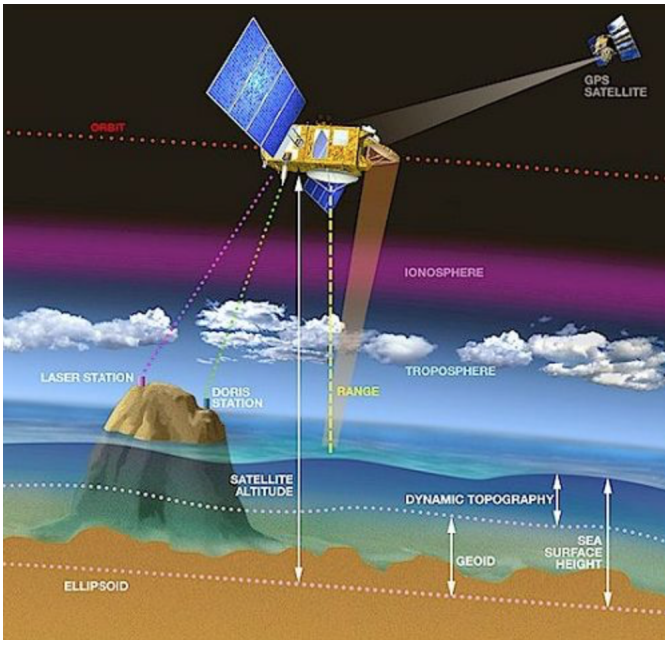

Figure 1: A illustration of the principle of satellite altimetry. Credits CNES/Ill. D. Ducros

The altimeter installed onboard Jason-3, is as previously mentioned, the Poseidon-3B altimeter, developed from the altimeters from its predecessors on Jason-2 and Jason-1. The position of the satellite and therefore also the satellite altitude with respect to the reference ellipsoid, is tracked with great accuracy by the Global Positioning System (GPS) satellites and the Doppler Orbitography and Radiopositioning Integrated by Satellites (DORIS). The DORIS is developed by CNES, the French space agency, and is a global network of beacons exploiting the knowledge of Doppler-shift, to determine the satellites orbital positions in space. The Earth based beacons are devices designed to attract attention to a specific location. A signal is emitted from the beacon and picked up by receiving satellites where from the change in frequency depending on the sources movement and position, can be derived and calculated into a velocity relative to the Earth (Rosmorduc et al., 2011). Figure 1 show an illustration of the principle of

the altimetry, including the DORIS station. In addition, the radar altimeter transmits waves at two separate frequencies; 13.6 (Ku band) and 5.3GHz (C band), making it possible to calculate the atmospheric electron content by comparing the path delay of the signal transmitted (Rosmorduc et al., 2011). The electron content in the atmosphere is proved to delay the return signal and distort the accuracy of the measurements. The following section, section 1.2, will introduce the applied corrections to the observed range necessary for high accuracy determination of in-land water level heights.

1.2 Applied corrections

To determine the water level height with the highest possible accuracy, necessary corrections to the measured data must be applied. The applied corrections fall into two categories; range corrections and geophysical corrections. Both groups of corrections will be presented below along with its typical values, subject to e.g. season of year or geographically latitude dependence.

1.2.1 Range correction

The range corrections adjusts the speed of the radar pulse, including dry-, wet- and ionosphere corrections. The corrected range, R_{corr} is related to the observed range, R_{obs}, as follows:

$$\mathrm{R}_{corr} = \mathrm{R}_{obs} - \Delta\mathrm{R}_{dry} - \Delta\mathrm{R}_{wet} - \Delta\mathrm{R}_{iono} \tag{1}$$

where $R_{obs} = ct/2$ is the measured range between the satellite and Earth's water surface, proportional to the speed of the radar pulse c and the travel time t. The sea surface height, h, above the reference ellipsoid, see Figure 1, is written as:

$$h = H - \mathrm{R}_{corr} = H - \mathrm{R}_{obs} - \Delta\mathrm{R}_{dry} - \Delta\mathrm{R}_{wet} - \Delta\mathrm{R}_{iono} \tag{2}$$

where H is the altitude of the satellite determined through orbit determination, with respect to the reference ellipsoid. The refraction from dry atmospheric gases ($\Delta\mathrm{R}_{dry}$) is clearly the most significant correction applied to the range, simple based on its mean value. It produces a nearly constant height error of approximately -2.3 m (J.P.Dumont et al., 2016). The dry troposphere refraction error has long spacial scales and is therefore not significantly influenced by land near coastal areas. However, the correction is only dependent on atmospheric surface pressure in mbar and latitude featuring highest values around the subtropical band and smallest values at high latitudes (O.B.Andersen and R.Scharro, 2011). Surface pressure is determined by the European Center for Medium Range Weather Forecasting (ECMWF) (J.P.Dumont et al., 2016).

The wet troposphere correction, $\Delta\mathrm{R}_{wet}$ is purely dominated by the water vapor in the troposphere, differing from the dry corrections mostly by its complexity due to high temporal variations in time and

space. In extremes, height calculation errors for dry, cold air is just a couple of centimeters to more than 30 centimeter in hot, wet air (O.B.Andersen and R.Scharro, 2011). The variations are especially observed in coastal regions, as well as for larger lakes, causing the correction to be less accurate with uncertainties of 1.5 cm against ∼0.8 cm at long distances from coastlines (J.P.Dumont et al., 2016). Weather prediction models, such as ECMWF, do provide values for wet troposphere, although it is preferable to calculate real errors obtained from an Advanced Microwave Radiometer (AMR) measuring the brightness temperatures offering almost direct measurements of wet troposphere corrections. Also the wet troposphere error is strongly dependent of latitude, with highest values in the equatorial band and lowest values by Antarctica, -30 cm and -5 cm respectively (O.B.Andersen and R.Scharro, 2011).

This leads us to the ionosphere refraction (ΔR_{iono}); the refraction of electromagnetic waves which is directly linked to the presence of free electrons in high altitudes about 100 kilometers. In these altitudes high energy photons emanating from the Sun are able to strip atomic and molecular gasses which interfere with the electromagnetic wave, or the radar pulse, causing a delay on the radar pulse. The perturbations acting on the signal is proportional to the electron density in the ionosphere, also referred to as the *total electron content* (TEC). TEC is dependent on season of year and solar activity (variations by a factor 5 between low ad high solar activity (Scahrroo and Visser, 1998), but is insensitive to coastlines. The altimeter may over-estimate the range to sea surface by 0.2 to 20 cm with accuracy ±0.5cm[1] (J.P.Dumont et al., 2016) .

1.2.2 Geophysical correction

The geophysical corrections are the most dominant contributors to the temporal water level height variations, which includes the tide corrections; load-, pole-, and solid Earth tide as well as the geoid model. The dynamic sea surface height, h_D, is expressed as follows:

$$h_D = h - h_{load} + h_{pole} + h_{solid} + h_{geoid} \tag{3}$$

The load tide, h_{load}, is synced with the ocean tide as it is driven by the ocean tide and is approximately 4-6 % of the ocean tide. The ocean tidal effect is due to the elastic response of the Earth's crust to ocean tides, producing deformation of the sea floor and a surface displacement of an adjacent land. (O.B.Andersen and R.Scharro, 2011). The value is computed and predicted by GOT4.8 and FES2004, finite-element hydrodynamic models, complying continuous input from tide gauges and altimeter data (J.P.Dumont et al., 2016).

Pole tide, h_{pole}, is the change in the centrifugal forces due to variations of the Earth's axis producing a signal in sea surface height at the an equal frequency. The magnitude of error is alleged to be insignificant (10^{-3}), however it must still be corrected for. The values are computed to high accuracy (O.B.Andersen

[1] at frequency 13.6 GHz, used by the Poseidon-3B altimeter mounted on Jason-3

and R.Scharro, 2011).

Lastly, the Earths response to external gravitational forces of the Sun and the Moon must be accounted for, h_{geoid}. It can be considered to be in equilibrium with the tide-generating forces to the surface i.e. the surface is parallel with the equipotential surface and tide height proportional to the potential. The ratio of those, represent the Love numbers. The correction is assumed to be highly accurate with solid Earth tide ranges, and up to ±20 centimeter (O.B.Andersen and R.Scharro, 2011).

The geoid, h_{geoid}, is a 'fictive' or modeled ocean surface, shaped as how the surface of the oceans would be under the influence of the Earths gravitation and rotation alone. The geoid undulations are given with respect to a geocentric reference ellipsoid. The reference ellipsoid is simply a mathematical defined surface which approximates the geoid. Where there is a positive gravity anomaly, the geoid is higher than the reference ellipsoid (up to 83 m) and wherever there is a negative anomaly the geoid is lower than the reference ellipsoid (down to 106 m) (J.P.Dumont et al., 2016). The anomalies are due to the inhomogeneity in the density of the Earth's interior and crust (O.B.Andersen and R.Scharro, 2011).

1.3 Altimetry crossovers

Single-and dual crossover data are formed at the geographical positions where ground tracks intersect and adds an extra possibility to validate altimeter system information (Schrama et al., 2000). Analysis of crossover height differences is a measure of geographically anticorrelated orbit errors, and is much useful for precise orbit determination. The method is simple and described as follows; (1) the location of crossing ascending and descending passes are determined, (2) the relative sea heights are most often converted back to range measurements by subtracting them from the orbital altitude and thereby (Scahrroo and Visser, 1998), (3) the difference between the ascending/descending passes is a reflection of the radial error. Equal errors or signals contained in either tracks forming the crossover, disappear at the crossover location (Schrama et al., 2000), as well as unalike signals are visible. Single crossovers differences are most widely used in relation with gravity model tuning, for tailored / improved gravity models, where dual satellites crossovers are most interesting for calibration matters between two missions. The dual satellite crossovers link the orbits in a common reference frame which may reveal gravity-induced effects that must be adjusted for. Obviously the accuracy at which the absolute sea level is inferred by differing the orbital altitude and altimeter range is limited by the accuracy of the orbit computation (Scahrroo and Visser, 1998). Mathematically, radial orbit errors of two crossing passes, can be expressed by the Linear Perturbation Theory. The theory describes the three orthogonal components of the orbit error as a linear combination of terms due to errors in the gravity model [2](Scahrroo and Visser, 1998).

[2]Linear Pertubation Theory will not be elaborated any further, since the crossover coefficients used in this rapport are automatically generated by RADS's max2 crossover generating program

2 Data for evaluation

In this section, the data selected and processed as part of this project, will be presented, highlighting that the actual data is included in section 4 as part of the results. This includes satellite data from Jason-2 and Jason-3 produced solely by *"Centre National d'Etudes Spactials"* (CNES) ((J.P.Dumont et al., 2016) and (J.P.Dumont et al., 2015)) and in-situ observations from a water station located at the inland lake of Vänern in Sweden accessed and reported by *"Sveriges meteorologiska och hydrologiska institut"* (SMHI).

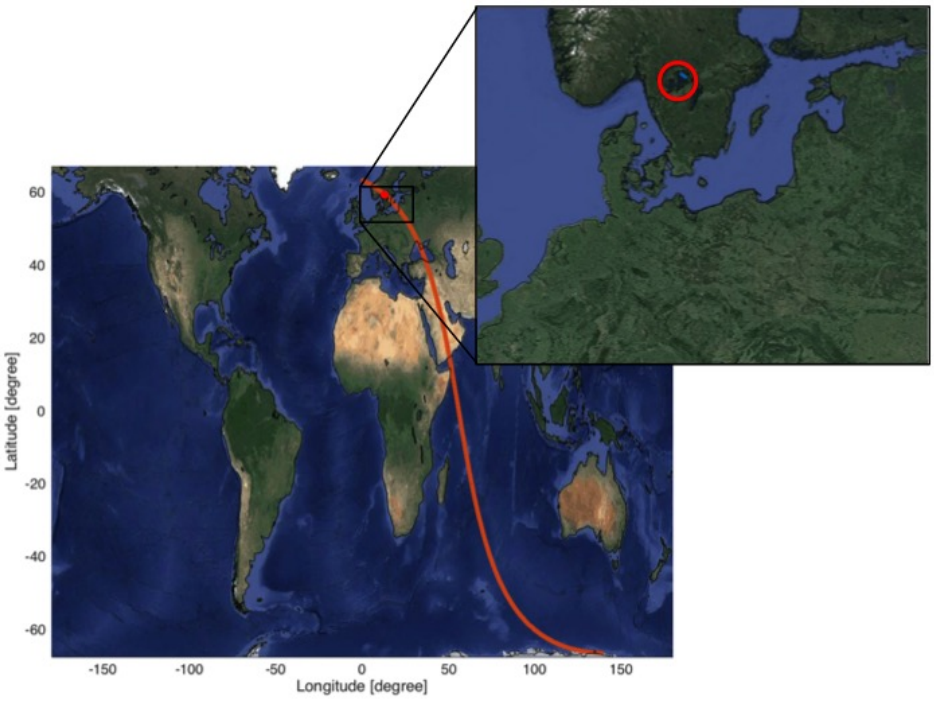

Figure 2: Ground track of pass 220, as well as Vänern (red cirkel) in Sweden and observation track (blue strip)

2.1 Satellite data

Jason-2 was launched in 2008 and has served scientist with important data to better understand the Earths hydrology system but the Jason-2 is now retiring so that the next generation satellite, Jason-3 can take over its place. The mission cooperative involves CNES, NASA and two additional participants, the *European Organisation for the Exploitation of Meteorological Satellites* (EUMETSAT) and the *National Oceanic and Atmospheric Administration* (NOAA). With an orbital altitude of 1336 km, Jason-3 is programmed to orbit identically to Jason-2 just one minute apart, operating at high inclination ($\pm$66.15 degree). An ascending pass begins at latitude -66.15 and ends at 66.15. A descending pass is the opposite. Both satellites complete a cycle of 254 passes (127 ascending and 127 descending), approximately every 10 days (J.P.Dumont et al., 2016). Practically, the data is retrieved from CNES via

aviso+'s ftp-server. Here Interim Geophysical Data Record (IGDR) is accessed, with the data format netCDF, containing both 1Hz records as well as 20 Hz high-rate values for almost all auxiliary data. 20 Hz data is used whenever available, simply due to 20 times as many data observations compared with the 1 Hz, otherwise 1 Hz will be interpolated. The cycles investigated are cycles 280 through 288 for Jason-2 and cycles 000 through 008 (cycle 000 through 007 for crossover), though it is only cycles 284 and 286 representing Jason-2 and cycles 004 and 006 representing Jason-3, that are detailed in this report. These cycles are chosen, since they represent their individual satellite observations, leading to a well defined calibration analysis. For convenience Jason-2 cycles will be referred to as 280, 281 and so on and similar Jason-3 satellite cycles will be referred to as cycles 000, 001 and so.

The large lake Vänern in southern Sweden, is chosen as calibration 'sight', since this meet the following criteria; firstly, the lake is great enough for a segment of an satellite pass (pass 220) to be selected without the footprint being influenced by land. See for instance Figure 2 for pass location and Vänern. Secondly, stationary water station observations are available. The water station measurements are obviously important as a reference point, when calibrating the Jason-3 data with the Jason-2 data to detect any similarities or the opposite in the satellite measurements observed.

2.2 Observations from water station

The in-situ data have been made available from the water station installed in the south of Vänern near the city of Trollhätten. From this station, a daily mean water level is observed, from 6.00am to 6.00am. The data information is public and can be reached from the SMHI open data service. The water level is measured with respect to Sweden's own reference system, RH2000, almost identical to the World Geodetic System (WGS84), and is expected to achieve very reliable measurements within an accuracy of only a few centimeters.

Table 1: The two reference ellipsoids and their characteristics; semi grand axe. (ESA, 2009)

Elliposid name	a (m)
TOPEX	637836.3
WGS84 (RH2000)	6378137

Most altimetery satellites, are computed relative to TOPEX ellipsoid, and so are the altimeters installed on Jason-2 and 3. In order to achieve the same level of reference, the mean water surface height observed by SMHI must be adjusted to successfully compare the in-situ observations together with the altimetry data. Table 1 scheme the semi-major axe properties for the mathematically defined reference ellipsoids. The difference between TOPEX and WGS84 is 70 cm, implying that the water station measures a water level with respect to a reference ellipsoid located 70 cm above the reference ellipsoid for Jason-2/Jason-3. Furthermore Sweden's height system, RH2000, is defined with respect to the Normaal

Amsterdams Pei (NAP) (Lantmäteriet, 2016), implementing 1 cm (BKG, 2016) to be subtracted in order to achieve the same level of reference. Consequently, 0.69 m must be added to the observed water surface height of the water station, to achieve the same level of reference.

3 Method and considerations

In this section the method of processing and handling the selected data will be outlined. The $Matlab\_R2015b$ has been applied as the main software to carry out the data processing. The Radar Altimeter Database System (RADS) has provided the crossover data (will be explained in section 3.2). Besides, Matlab-scripts belonging to the respective sections below, are attached in Appendices.

3.1 Processing of satellite data and water station measurements

The netCDF file contains 177 columns of data, where of course only a handful of these are applicable for this project, including range, altitude, the various corrections and the geoid model, EGM96. The range- and geophysical corrections are done in same order as presented in the theory, section 1.1. See appendix B.1 for Matlab-code. Across the lake, Vänern, an average of 73 observations points are collected. To asses a reasonable calibration test of the Jason-3 data the mean value or/and the standard deviation are typically good indicators. However these indicators may be quite sensitive to off-sets (depending on number of observations points, compared to off-sets), decreasing the reliability of the estimated parameter. In such case, corrected water level heights not meeting the stated condition below, will be assigned "not-a-number" (NaN), and will be disregarded:

$$|x_n - \bar{x}| > |3 * \sigma(x_n)| == NaN$$

This condition or criteria is commonly utilized to discharge outliers and achieve a more general and homogeneous data set and therefore better estimates of statistical mean and standard deviation representatives for the specific area. The condition has been repeated three times, but may be performed as many times as necessary until value changes are very little. The computed values for each cycle of both satellites are listed in Tabel 2. Subsequently, the calculated mean values of each cycle are held up against the in-situ measurements for direct comparison. See appendix B.2 for Matlab-code. The water station observations are loaded from a publically accessible .xls-file, making it very easy to utilize in the calibration process. Additionally, mean values of sets of 20 points for each satellite cycle (pass 220 across Vänern) is computed. This is an American approach to calibrate and estimate similarities and results listed in Tables 4 and 5.

3.2 Single- and dual crossover

The extensive altimetry crossover in the Jason-2 and Jason-3 missions is to calibrate the accuracy of Jason-3. The primary data are crossover differences, both single- and dual within and between Jason-2 and Jason-3 missions. Specially, dual satellite crossover is an efficient test of Earth gravity-models and to detect relative coordinate sysstem offsets between less precise and more accurate orbits of altimetry missions like Jason-3 and Jason-2. The crossover data is simply computed via RADS, being an internet facility operating within the framework of the Netherlands Earth Observation NETwork and establish validated and cross-calibrated altimeter data (Naeji et al., 2000). The crossover locations and related statistics are found by performing the crossover generating program; *max2*(Scharroo, 2012), identifying relevant single and dual crossovers. The crossovers have been averaged in latitude bands of 1 degree, in order to interpret the sea level anomaly (and significant wave height) latitude-sensitivity profiles, in order to show eventual evidence of anticorrelated geopotential signals due to any geodetic offsets.

4 Results and calibration

In this section the outcome of the applicable data processing will be presented. Firstly, assembled Jason-3 data is compared with Jason-2 data in section 4.1. Subsequently in section 4.2, means of every 20 observations points across Vänern are derived, and thus compared with in-situ measurements. Lastly single- and dual satellite crossover data is presented in section 4.3, where also statistical results are listed; number of crossovers (XO's) processed, mean values, standard deviation (st.d.) and root mean square (rms).

4.1 Jason-3 observations compared to Jason-2 observations at Vänern

Mean values and standard deviations, as well as number of observation points from the satellite data included in this assessment, are tabled in Table 2. The blank labels are due to missing data of the particular pass in the respective cycle. It is noticed how the mean values of the two satellites measure absolute differences around 2-3 cm, with Jason-2 measuring the slightly higher elevation of the Vänern water level. For all the considered cycles, the standard deviation is 5-7 cm indicating homogeneous results. Results representing the eighth cycle for either satellites (287/007), deviate much from the other cycles. The reason is most likely a combination of correction errors and bad weather, affecting the range measurements, resulting in many not-a-number (NaN) indices. This is also reflected in the very high standard deviation. The same reason is assumed to apply for cycle 283. These results are not believed to be representative for the mean water level height derived by Jason-2 and 3, and are excluded in the overall calibration analysis, however the outlying results are yet included in the table for information.

Table 2: Statistic of altimetry data across the lake, Vänern. J2 and J3 are just abbreviations for Jason-2 and Jason-3. The date is written as (mm.dd) and n is the number of selected observations within the set boundary of Vänern. The last column, gives the absolute difference and values denoted (*) are included for completeness. All values are in meters.

Date	n	cycle nr. (J2)	mean	st.d.	n	cycle nr. (J3)	mean	st.d.	J2-J3
02.16	74	280	44.8035	0.0825	73	000	44.7970	0.0605	0.0065
02.25	74	281	44.7846	0.0738	73	001	44.7547	0.0564	0.0299
03.06	74	282	44.7364	0.0557	72	002	44.7176	0.0734	0.0188
03.16	74	283	39.8436*	3.8627*	-	003	-	-	-
03.26	73	284	44.7366	0.0604	75	004	44.7069	0.0649	0.0297
04.05	-	285	-	-	76	005	44.7132	0.0737	-
04.15	74	286	44.7616	0.0681	65	006	44.7327	0.0599	0.0289
04.25	73	287	43.3978*	2.0736*	76	007	42.8069*	2.5951*	0.5909
05.05	73	288	44.8167	0.0668	75	008	44.790	0.0615	0.0227

4.2 Water station measurements compared to satellite observations

Below, Table 3, lists the absolute differences between altimeter observations derived by Jason-2 and Jason-3 (same mean values as listed in Table 2) and in-situ measurements, from the water station in Vänern. The relative differences between the *J3-water station* and *J2-water station* are of course identical with the mean differences in Table 2. It is noticed how Jason-3 observe a water level height approximately 33 cm lower than the water station (Jason-2 observe approx. 30 cm lower than the water station), thus reflecting the average difference of approx. 2-3 cm between the respective satellite measurements, with Jason-2 giving the higher water level observation. It is justifiable assumed that the water station measures the "true" water level height, this being the reference and benchmark measurements in this comparison of the Jason-3 versus Jason-2 measurements.

Table 3: Absolute differences between altimetry observations of Vänern (for J2 and J3) and in-situ measurements by water station. J2 and J3 are just abbreviations for Jason-2 and Jason-3. Values denoted (*) are included for completeness. All values are in meters.

date	cycles (J2/J3)	water station	J3 - water station	J2 - water station
02.16	280/000	45.11	-0.3130	-0.3065
02.25	281/001	45.09	-0.3353	-0.3054
03.06	282/002	45.08	-0.3624	-0.3436
03.16	283/003	45.06	-	-5.2164*
03.26	284/004	45.03	-0.3231	-0.2934
04.05	285/005	45.02	-0.3068	
04.15	286/006	45.07	-0.3373	-0.3084
04.25	287/007	45.11	-2.3031*	-1.7122*
05.05	288/008	45.13	-0.3360	-0.3133

The two following tables, Table 4 and Table 5 simply list mean values of every set of 20 ground track observation points detected across Vänern by pass 220. Expectedly, the mean values of each interval do not deviate significantly from the previous set of points, with exception of cycle 283 and cycle 287.

(Without further notice, the water level heights observed for 287 and 007 are graphed with respect to longitude, pictured in appendix A.1 together with cycle 006 for reference). The mean values (three values pr. cycle) are plotted in Figure 3 together with water level heights registered by the water station, for comparison. Overall differences represented in Figure 3, correspond well with the differences listed in Table 3. Outliers are eliminated from the plot by the y-axis settings.

Table 4: Averaged Jason-2 ground track observations of every 20 observations of a total of 60 data points (20 x 3). Values denoted (*) are included for completeness. All values are in meters.

Obs. points	280	281	282	283	284	285	286	287	288
1-20	44.8190	44.7706	44.7364	36.8327*	44.7447	-	44.7564	44.9667	44.7974
21-40	44.7715	44.7777	44.7425	NaN*	44.7305	-	44.7760	41.6834	44.8389
41-60	44.8198	44.7315	44.7315	NaN*	44.7316	-	44.7504	44.4603	44.8173

Table 5: Averaged Jason-3 ground track observations of every 20 observations of a total of 60 data points (20 x 3). Values denoted (*) are included for completeness. All values are in meters..

Obs. points	000	001	002	003	004	005	006	007	008
1-20	44.7939	44.7426	44.6976	-	44.7005	44.7480	44.7275	-	44.7991
21-40	44.7734	44.7402	44.7344	-	44.7107	44.7061	44.7221	42.0483	44.8031
41-60	44.8019	44.7668	44.7140	-	44.7031	44.7036	44.7484	36.9833*	44.9899

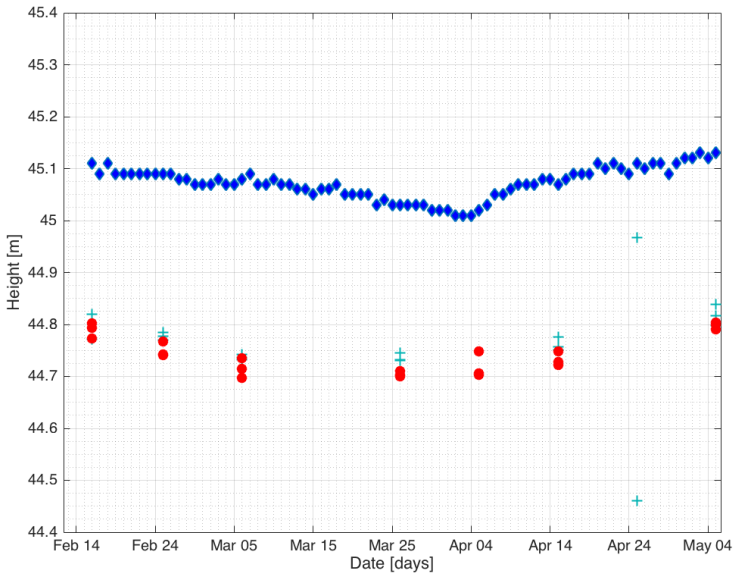

Figure 3: Water station height (diamonds), water level height derived by Jason-2 (+) and water level height derived by Jason-3 (○)

4.3 Single- and dual crossover results

Along the Equatorial band, primarily in the mid Pacific- and in the Atlantic ocean areas, less crossovers are determined, as seen for the representative single satellite crossovers for cycles 284 and 004 (Jason-2 and Jason-3 respectively) plotted in Figure 4. The much larger scales around the Equator, is in contrast to the natural regular "grid", which the crossovers form with increasing density towards the poles. Minor areas free of crossovers are observed north-east of Australia in the Coral sea (Great Barrier Reef), near the coastline east of South-America bounding the North-Atlantic Ocean and a in the Indian Ocean east of Madagascar. Globally, the crossover results shows that the overall sea level anomaly differences are dominated in the range -2 cm to 2 cm, based on the representative scatter plots. In below section 4.3.2, statistical values coupled with the generated crossover determinations are shown.

Single satellite crossover locations for representative cycles 286 and 006 are presented in Figure 5. Based on these scatter plots, it seems as if there are noticeable less crossover locations than as presented in Figure 4. This turns out not to be the case. Table 6 and Table 7 in section 4.3.2, list number of single satellite crossovers determined; cycle 286 determine around 500 more XO's than cycle 284, and roughly 180 more XO's are determined in cycle 006 for Jason-3 than for cycle 004. This seems to be inadequately represented from viewing. It is also recognized how the same regions, which are free of XO's, are pronouncedly devoid, as for Jason-2 cycles 284 and 004. Further, a great area of the Indian Ocean east of Africa is free of crossovers, with only little crossover locations. In the coastal regions, for instance in the waters of Indonesia, less XO's are located only with few distinct locations. It is expected of Jason-3 to better measure coastal areas, because of the improved altimeter, capable to switch automatically between two modes[3].

The generated crossover locations of the dual satellite differences are displayed in Figure 6. It is noted, that the XO differences seems to be dominantly labeled red, representing observations roughly between 6 cm and 10 cm, indicating that Jason-3 measure a lower sea level anomaly compared to Jason-2. Designated areas seen, in Figure 6a, near the coastlines of South-America, south of Africa and in north Australia XO differences reach values between -4 and -8 cm, which indicates that in these areas the Jason-3 satellite measures a higher sea level anomaly compared to the Jason-2 satellite. Figure 6b also reveal significant negative differences in coastal regions, though limited to the coast near the Netherlands, India and South Africa.

[3] 1st mode: speeds up the acquisition of the surface. 2nd mode: the satellite to surface distance will be estimated by the altimeter using the real-time orbit position predicted by DIODE (on board navigator based on DORIS receiver) and using the elevation of the surface stored in a DEM (Digital Elevation Model) within the altimeter (NOAA et al., 2015)

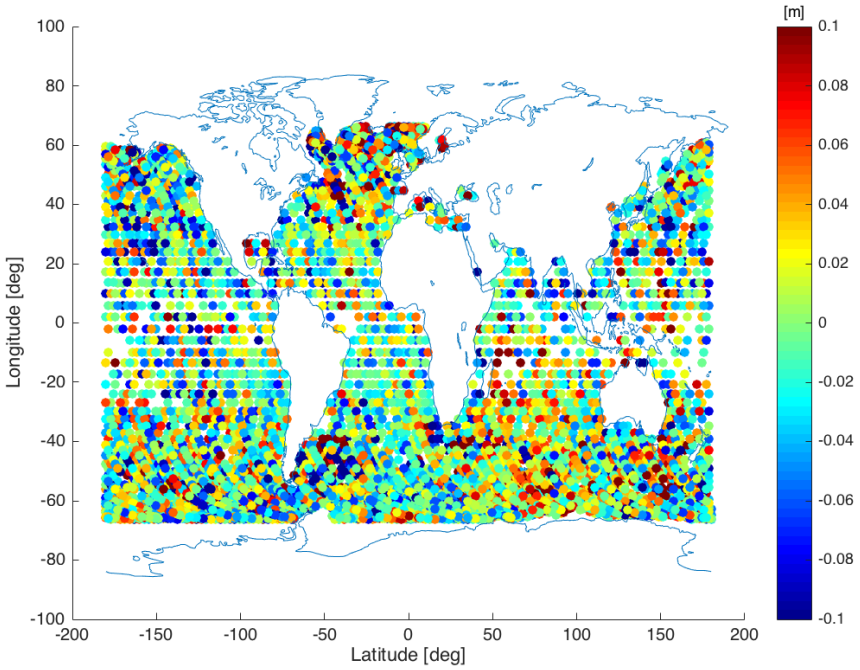

(a) Single satellite crossover for Jason-2, cycle 284

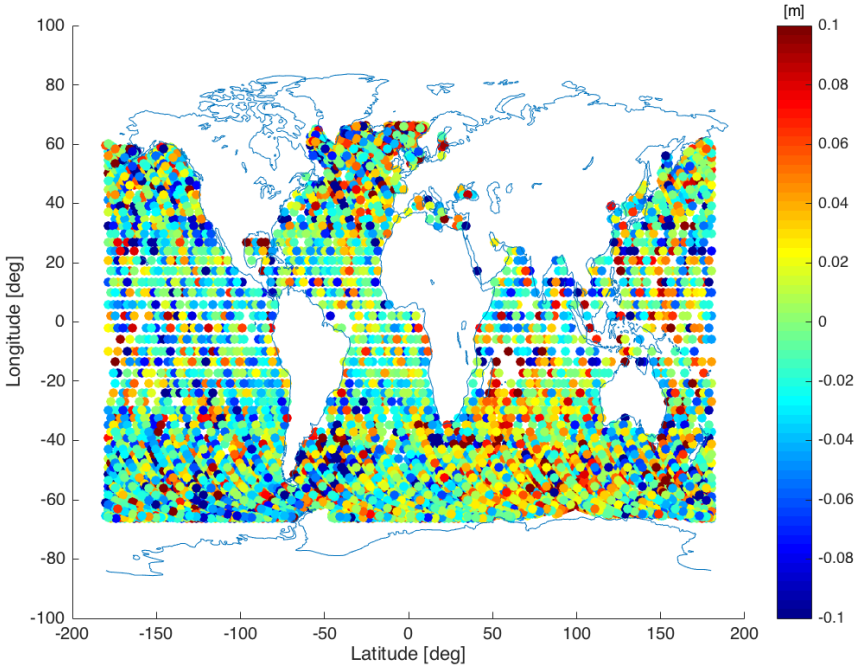

(b) Single satellite crossover for Jason-3, cycle 004

Figure 4: Averages of Jason-2 and Jason-3 single mission crossover differences. The graphs show: 4a) for cycle 284 and 4b) for cycle 004.

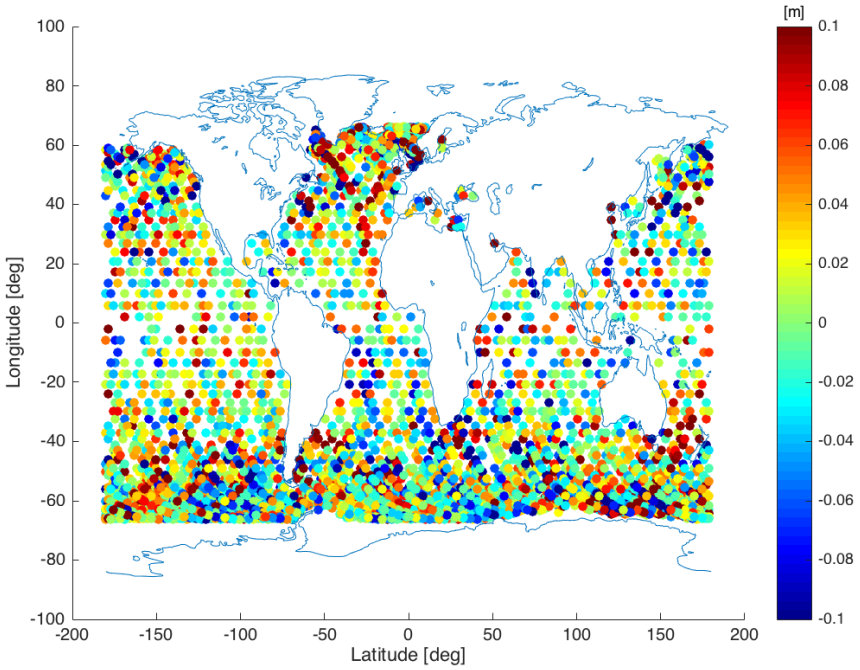

(a) Single satellite crossover for Jason-2, cycle 286

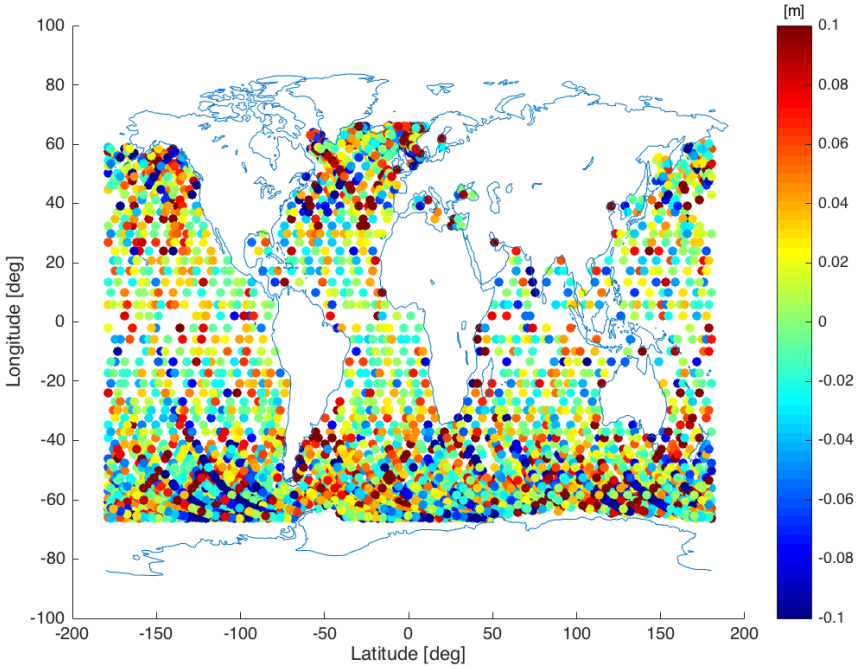

(b) Single satellite crossover for Jason-3, cycle 006

Figure 5: Averages of Jason-2 and Jason-3 single mission crossover differences. The graphs show: 5a) for cycle 286 and 5b) for cycle 006

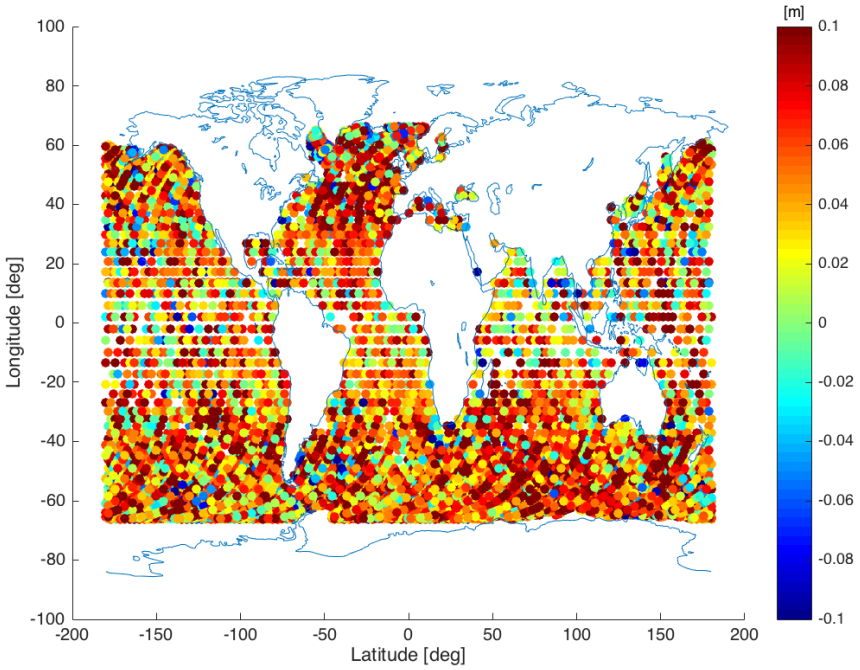

(a) Dual satellite crossover for cycle 284/004

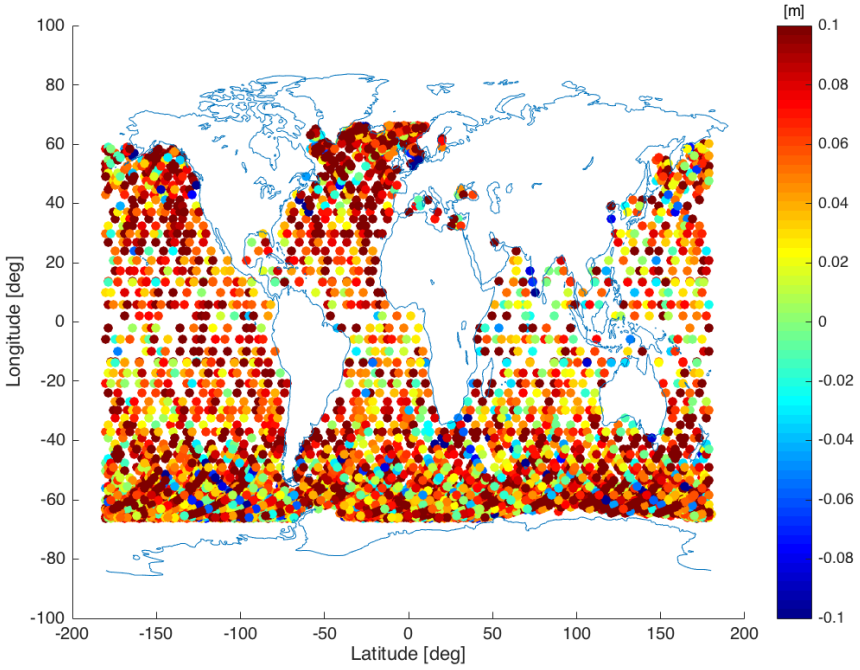

(b) Dual satellite crossover for cycle 286/006

Figure 6: Locally averaged dual-satellite crossover differences (Jason-2 minus Jason-3) of sea level anomaly. The graphs show: 6a) for cycle 284/004 and 6b) for cycle 286/006

4.3.1 Collinear profiles

Figure 7 gives an example of a pair of collinear tracks of Jason-2 and Jason-3 (cycles 284 and 004 respectively), with a 1-minute time difference. Figure 7a gives the sea level anomaly for both collinear tracks as well as the dual satellite crossover. It is noted how they correlate nicely, only with noticeable differences around the 50 degree latitude. More interesting are the differences for the dual satellite XO's. Here is observed an overall shift of about 4.5-6 cm and a minor "bulge" is shown at the Equatorial band mainly between the -10 and 10 degrees latitude. The "bulge" is tending toward lower difference in sea level anomaly. Figure 7b depicts the differences in observed significant wave height for both collinear tracks; single- and dual. It is noted, to see more identical significant wave heights (SWH) near the Equatorial plane (ranging around 0 m), than near the poles (ranges within $0.5-0.15$ m). As for the SWH, dual crossovers are shifted to the left giving negative differences all around, indicating that Jason-3 measure a SWH higher than Jason-2. It may be considered to suggest an interrelation between the two parameters; Figure 8 present coherency between dual XO differences in significant wave height and dual XO differences in sea level anomaly. The linear fit is $y = 0.16x + 0.049$. The slope equal to 0.16 is a result of sea level variability as a function of the SWH. On the other hand, it is noted, that the scatter of results shown in Figure 8 is significant, thus providing a fairly uncertain representation of a linear by regression analysis.

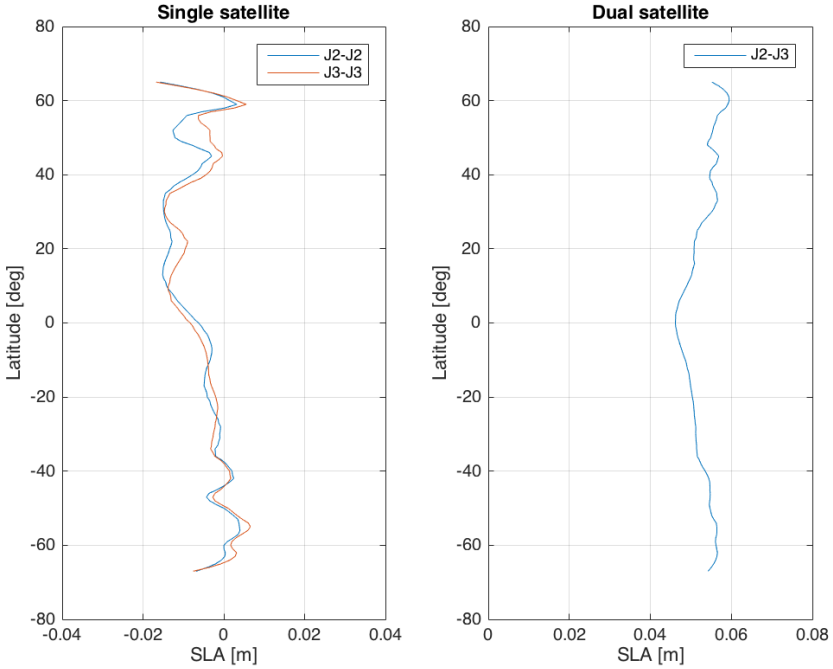

(a)

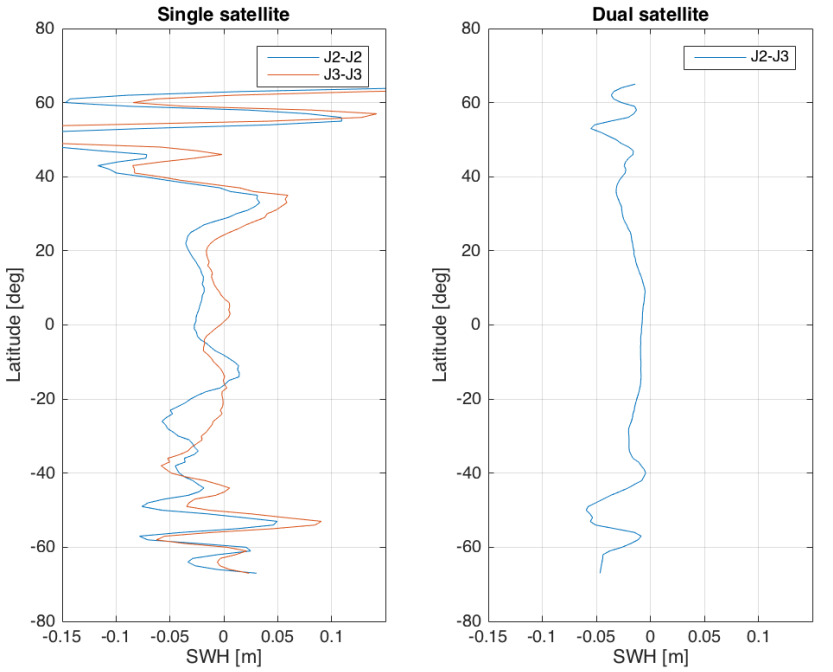

(b)

Figure 7: Figure 7a) show single- and dual satellite crossovers in averaged latitude bands for the collinear tracks; Jason-2 cycle 284 and Jason-3 cycle 004. Figure 7b) show averaged SWH ordered in latitude bands of 1 degree latitude, for the same collinear tracks.

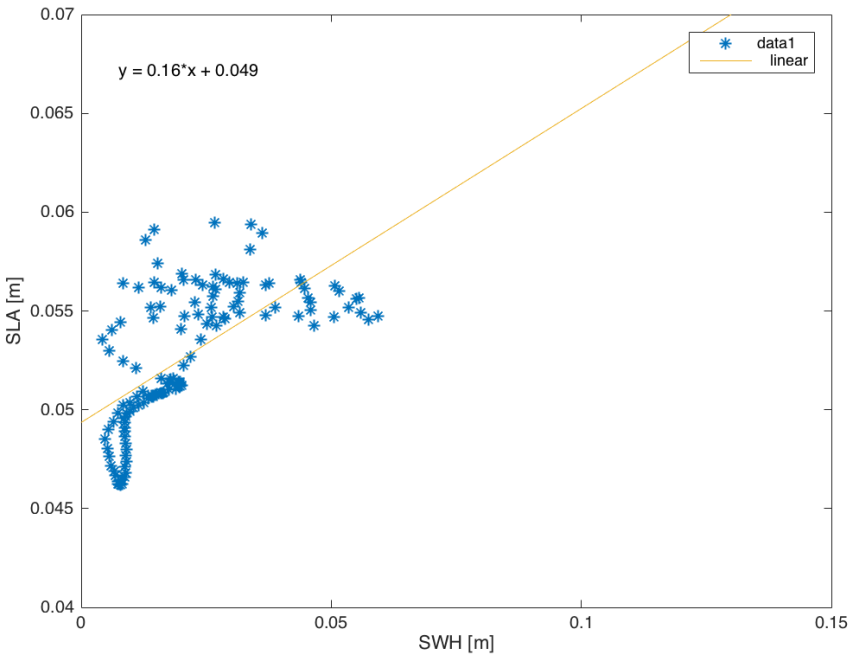

Figure 8: A linear regression relating dual satellite crossovers differences of sea level anomaly with (dual) crossover differences significant wave height for cycles 284 and 004.

The sea level anomaly profile presented for both single- and dual satellite XO's (cycle 286/006) in Figure 9a are quite similar to those in Figure 7a. Once again, the "bulge" near Equator is clearly seen, even more significantly than for the collinear tracks represented for 284/004. Expectedly, the decrease in sea level anomaly near Equator correspond to the less turbulent significant wave height in the same region, at least compared to the poles. The dual satellite crossover due to significant wave height reach maximum values up to about 8 cm in northern latitudes and a minimum of -5 cm is reached close to Antarctica. By the Equator, ± 20 degree latitude, the differences ranges between 0-2 cm from 0 cm differences. Figure 10 link the SWH and SLA resulting in a linear equation equal to $y = 0.13x + 0.05$.

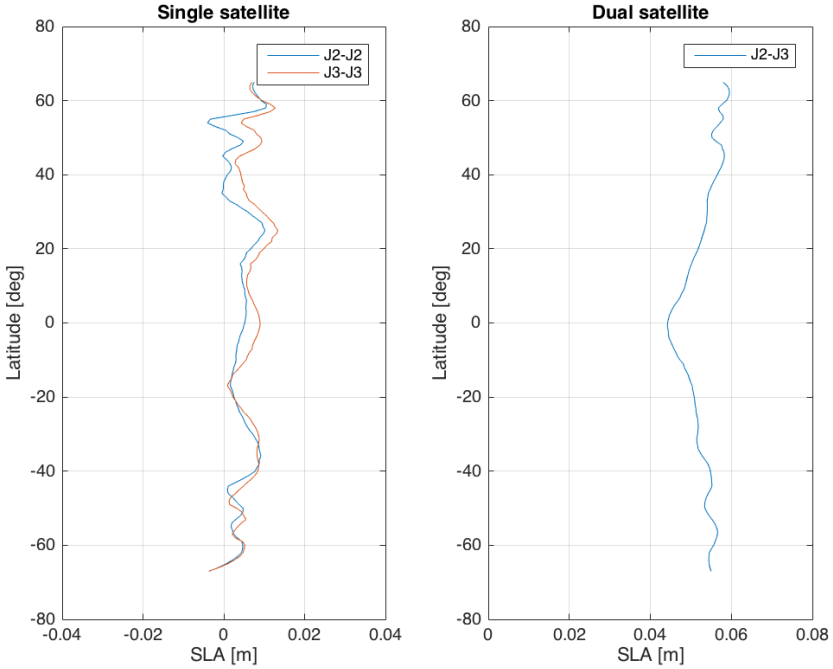

(a)

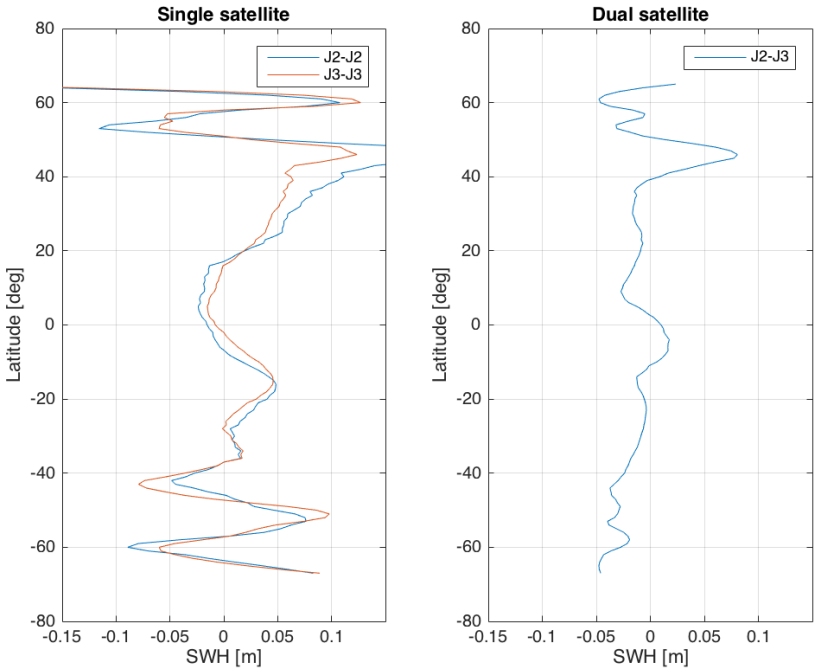

(b)

Figure 9: Figure 9a) show single- and dual satellite crossovers in averaged latitude bands for the collinear tracks; Jason-2 cycle 286 and Jason-3 cycle 006. Figure 9b) show averaged SWH ordered in latitude bands of 1 degree latitude, for the same collinear tracks.

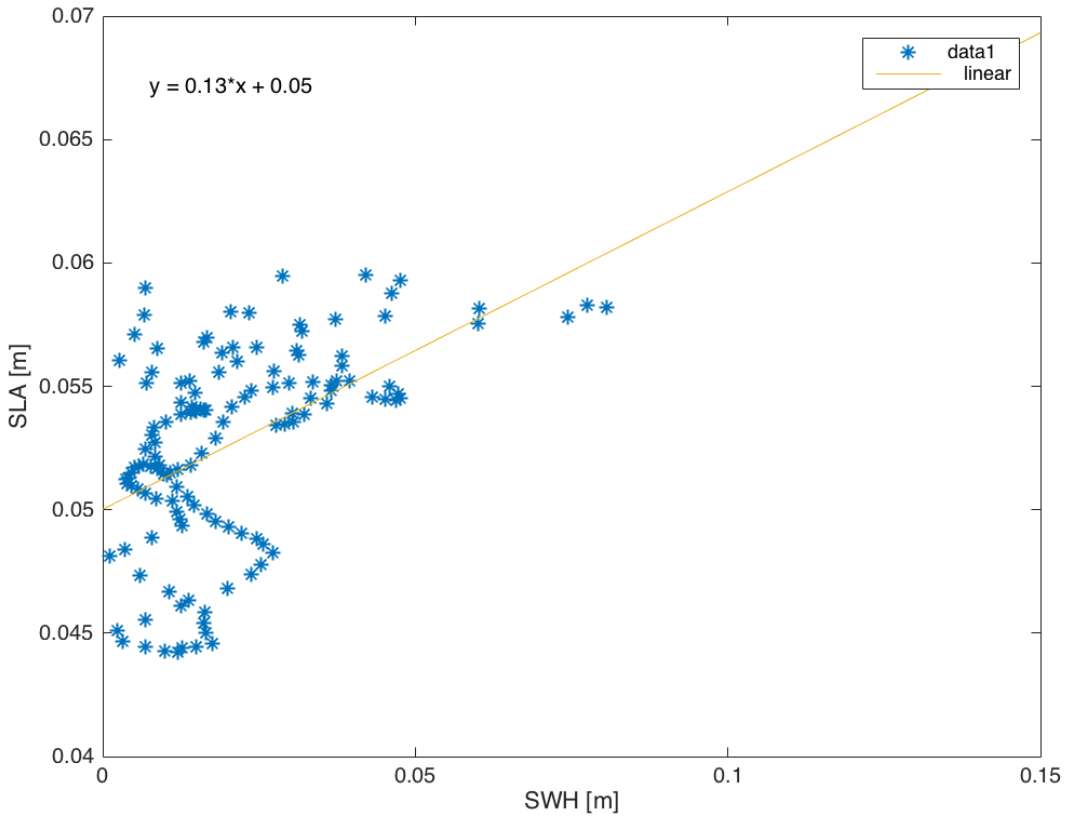

Figure 10: A linear regression relating dual satellite crossovers differences of sea level anomaly with (dual) crossover differences significant wave height for cycles 286 and 006.

4.3.2 Crossover statistics

For comparison of the crossover statistics for the applicable satellites, the values determined for Jason-2 is set as reference, against which, the Jason-3 values are compared for calibration.

Based exclusively on the st.d. values between the single satellite crossover observations, the Jason-2 seem to be slightly more accurate, see Tables 6 and 7. For example; cycle 284 calculate a standard deviation equal to 5.538 cm, whereas the comparative Jason-3 cycle, calculate a st.d. equal to 5.589 cm, corresponding to a relative difference of 0.90%, compared to Jason-2. The relative differences between cycles 282/002, 286/006 and 287/007 are 1.6%, 0.67% and 0.80%, respectively. Relative changes of cycles 280/000, 281/001, 283/003 and 285/005 are excluded, since (1) cycle 000 and 001 are considered to be uncertain, based on number of processed XO's and (2) cycle 285 and cycle 003 are both missing several passes, due to instrumental calibration, making these statistical values doubtful. However for the sake of good order, the statistics of these cycles are still schemed for information.

Table 6: Sea level anomaly differences of single crossover for Jason-2 alone. Values (*) are derived with much less crossovers due to less pass's. All values are in centimeters.

cycles (J2)	280	281	282	283	284	285	286	287	288
Nr. of XO	7304	7316	7260	7225	6773	5672*	7312	6781	6673
mean (cm)	-0.246	0.153	0.309	0.484	-0.29	0.103*	0.306	0.189	0.307
rms (cm)	5.112	5.221	5.194	5.232	5.546	5.269*	5.707	5.532	5.706
st.d. (cm)	5.106	5.219	5.184	5.209	5.538	5.268*	5.698	5.529	5.698

Table 7: Sea level anomaly differences of single crossover for Jason-2 alone. Values (*) are derived with much less crossovers due to less pass's. All values are in centimeters.

cycles (J3)	000	001	002	003	004	005	006	007
Nr. of XO	1668	6160	6234	4031*	7414	7456	7590	5894
mean (cm)	0.086	-0.11	-0.077	0.385*	-0.159	0.120	0.429	0.327
rms (cm)	4.877	5.572	5.269	5.643*	5.591	5.483	5.752	5.583
st.d. (cm)	4.876	5.570	5.269	5.629*	5.589	5.482	5.736	5.573

As for the statistics related to the dual satellite crossovers, see Table 8, the mean values for cycles 284/004 and 286/006, are 2.609 cm and 2.898 cm respectively, agreeing well on the st.d. resulting in 6.255 cm and 6.257 cm. On the other hand, note how the collinear tracks of cycles 284/004 determine almost 1500 less crossovers than for cycles 286/006. The number of crossovers found for each respective cycles is typically used as an additional parameter, and important to take into account, when analyzing the significance of the calibration.

Table 8: Dual satellite crossover differences of sea level anomaly between Jason-2 and Jason-3. Values (*) are derived with much less crossovers due to less pass's. All values are in centimeters.

cycles (J2/J3)	280/000	281/001	282/002	283/003	284/004	285/005	286/006	287/007
Nr. of XO	15947	26876	26936	22053*	28348	26132	29789	25318
mean (cm)	2.376	2.729	2.752	2.856*	2.609	2.742	2.898	2.969
rms (cm)	6.398	6.664	6.480	6.621*	6.777	6.604	6.895	6.848
st.d. (cm)	5.941	6.080	5.867	5.973*	6.255	6.008	6.257	6.171

5 Discussion

In this section the results as describes in section 4 above, will be discussed in the context of Jason-3 calibration against Jason-2. Generally, the global analysis permitting the assessment of the overall accuracy as well as latitude-dependent characteristics, are exclusively based on cycles 284 and 286 from Jason-2 and cycles 004 and 006 from Jason-3. The comparison of Jason-3 against Jason-2 with the water station as benchmark, is based on an overall evaluation of the results listed in Tabel 3 (and seen in Figure 3), providing a number of 8 cycle measurements for each of the satellites.

Overall, the Jason 3 results for both the Vänern and the crossover comparisons, shows good alignment with the Jason-2 results, with the more detailed findings highlighted below. It has not been possible, based on the data processed, to identify a distinct improved accuracy of the Jason-3 measurements compared to Jason-2, as concluded from the calibration of data with the Vänern water station. But it is believed to be justified from the results presented, that the Jason-3 data are to a high degree, comparable with the results seen from its predecessor Jason-2. It is noted, that the calibration performed, are based on a very limited set of data, and that more substantial processing of Jason-3 data over its mission period of approximately 5 years, may reveal more significant evidence of the improved measurements Jason-3 is capable of, compared to Jason-2.

5.1 Jason-3 compared to Jason-2 at Vänern

Across the short ground track of Vänern, the mean values extracted by the small collection of altimetry observations, suppose that Jason-3 measure a water level height 2-3 cm lower than the Jason-2 satellite with equal accuracy represented by the similar of st.d. 6 - 7.5 cm. Thus, the accuracy of the Jason-3 results shows very good alignment with the accuracy of measurements observed by Jason-2, at the geographical location of Vänern.

5.2 Water station compared to satellite observations

In extension to the previous section it is relevant to have a reference point(s), to put the satellite observations in perspective relative to the actual water level height measured by the water station. Figure 3 graphs the three "observer's" and interestingly neither of the radar altimeters measure a water level height equal to the water station. Likely, the offset of 30-33 cm is due to error in the corrections, over estimating the satellite to surface range. Thus, an improved match by Jason-3 with the benchmark water station data compared with Jason-2, has not been achieved with the cycles and data processed.

5.3 Calibration on single crossover differences

The global analysis of single crossover data are profitably used to valid errors of individual satellites alone, but is even more widely used to enhance the effect of orbital satellites and reduce errors and biases that do not change within the duration of one cycle(Klokočnik et al., 1999).

Separately, the satellites seem well correlated despite the somewhat chaotic pattern of small local variation. Tables 6 and 7 assist with mean values of the sea level anomaly ranging within 0.15-0.3 cm. However, in terms of accuracy, Jason-2 compute a standard deviation marginally better than Jason-3 (relative difference of 0.7%-0.9%).

The areas free of crossovers for Jason-2 recur in Jason-3, possible indicating lack of parameters for model corrections, or range measurements strongly contaminated by land or weather, such that observations are disregarded in the crossover locations. Likewise, areas free of crossovers, are close to land, which yet just emphasize the challenges related to altimetry and complex models. However Jason-3 is expected reduce the effects of thus problem in coastal regions, due to its altimeter Poseidon-3B; coupled with DORIS/DIODE to improve measurement capability over coastal areas, inland waters, and ice surfaces (NOAA et al., 2015). The profiles of crossovers (SLA) averaged in latitude bands from Jason-2 alone and Jason-3 alone correlate nicely, indicating less range distributions in these areas.

More interestingly are the results of dual satellite crossovers. A justifiable assumption is that Jason-2 orbit errors are smaller compared to those of Jason-3, such that the Jason-2/Jason-3 dual satellites crossover differences display Jason-3 errors rather than errors caused by Jason-2 ((Scahrroo and Visser, 1998)).

As Scahrroo and Visser (1998) phrases it: *"only when the precise orbit determination is stretched to its limit, ERS-2 altimetry will be regarded a reliable source of information, able to demonstrate its additive value in ocean research and unique capabilities"*. The second European Remote Sensing satellite (ERS-2) was launched in the mid 90's to orbit its predecessor ERS-1 by 32-hours, using crossover differences for calibration. The situation is similar to the case of Jason-2 and Jason-3, so it was found appropriate to rephrase the phrase so that it matched to the Jason-3. Likewise, a justifiable assumption is that Jason-2 orbit errors are smaller compared to those of Jason-3, such that the Jason- 2/Jason-3 dual satellites crossover differences, presented next, display Jason-3 errors rather than errors caused by Jason-2 ((Scahrroo and Visser, 1998)).

5.4 Calibration on dual crossover differences

As referred before, the dual crossover data from Jason-2/Jason-3 may tell little detail about the quality of the Jason-3 orbits. The crossover locations figured in Figure 6, conspire well with the collinear tracks, clarifying a geodetic offset between the missions. Klokočnik et al. (1999), outline the benefits of the dual crossover data; biases of the media corrections are fully exposed. Their research about TOPEX's

radial accuracy also include the theory of geopotential harmonics, making their calibration method more detailed. This will be suggested as future work, for further analysis of the Jason-3 data. Never the less, the mean values associated with the dual crossover height differences, showing mean values between 2-3 cm and standard deviation of roughly 6.2 cm seem to agree well with the collinear profile for dual satellite. Consequently, the latitude sensitive graph based on sea level anomaly, observing the shift of 4-6 cm to the right, well indicates that the Jason-3 satellite measures a lower sea level anomaly compared to Jason-2. Furthermore, equally interesting is the bulge observed ± 20 degree latitude of Equator, indicating lower biases in this band. Simultaneously, the differences in significant wave heights are observed to be less variable in the same zone and more turbulent close to the poles, initiating an expected, although uncertain coherence between the two parameters. The higher the significant wave height, a correspondingly high sea level anomaly is measured.

6 Conclusion

This report has aimed to calibrate the Jason-3 against the Jason-2, based on a limited selection of cycles including data from the in-land lake of Vänern and from global single- and dual satellite crossovers. As the two satellites have similar on-board altimetry equipment, the measurements being part of the calibration, are expected to be quite similar with potentially minor differences due to enhances technology developments in Jason-3.

The overall alignment of results from Jason-3 relative to Jason-2, is believed to be confirmed by primarily the benchmark calibration with the Vänern water station, where Jason-3 measures a water level height 2-3 cm lower than for Jason-2, yet as expected. Jason-3 measures with equal accuracy of 6-7.5 cm in standard deviation. However in extension to this, there is an off-set of 30-33 cm between the satellite measurements and the in-situ water station observation. This is believed to be due to inadequate accuracy in the applied corrections. Subsequently, analysis of single - and dual crossover differences underline that Jason-3 do measure a moderately lower sea level anomaly compared with Jason-2, measuring a sea level anomaly 2-3 cm lower than Jason-2 with an average standard deviation of 6.2 cm. Conclusively, Jason-3 perform with equal accuracy against Jason-2, though with an observed difference in mean water level observation of 2-3 cm across Vänern.

Furthermore, the sea level anomaly differences in the dual crossover locations, are latitude dependent, and seem to coherence with measured differences i significant wave height. By the Equatorial plane, differences in sea level anomaly is generally small ($\sim$ 0 cm), subject to minor variations in significant wave height in same zonal plane. Near the poles, the coherence is equally observed; high significant wave height differences toward the poles, provoke higher differences in sea level anomaly in the same regions.

The importance of achieving high accuracy results from the ocean surface height measurements,

stimulates the further enhancements in measurement calibrations as well as technology improvements, which for this Jason-3 calibration against Jason-2, may include significantly more data processing for improved knowledge of accurate corrections, more information on the information to be derived from crossover data as well as more reliable correlation between sea-level height anomalies and significant wave height measurements.

References

BKG (2016). Europäisches höhenreferenzsystem.

ESA (2009). Goce user toolbox (gut).

J.P.Dumont, V.Rosmorduc, L.Carrere, N.Picot, E.Bronner, A.Couhert, A.Guillot, S.Desai, H.Bonekamp, J.Figa, R.Scharroo, and J.Lillibridge (February 2016). Jason-3 products handbook.

J.P.Dumont, V.Rosmorduc, L.Carrere, N.Picot, E.Bronner, A.Couhert, S.Desai, H.Bonekamp, J.Figa, R.Scharroo, and J.Lillibridge (May 2015). Ostm/jason-3 products handbook.

Klokočnik, J., Wagner, C., and Kostelecký, J. (1999). Spectral accuracy of jgm3 from satellite crossover altimetry. pages 138–146.

Lantmäteriet (2016). Rh2000.

Naeji, M., Schrama, E., and Scharoo, R. (2000). The radar altimeter database system project rads.

NOAA, EUMETSAT, CNES, and NASA (2015). Jason-3. poseidon 3b altimeter.

O.B.Andersen and R.Scharro (2011). Range and geophysical corrections in coastal regions: And implications for mean sea surface determination. pages 103–145.

Rosmorduc, V., Benveniste, J., Lauret, O., Maheu, C., Milagro, M., and Picot, N. (2011). (5.) radar altimetry tutorial (rat).

Scahrroo, R. and Visser, P. (1998). Precise orbit determination and gravity field improvement for the ers satellites.

Scharroo, R. (2012). *RADS Version 3.1:User Manual and Format Specification.*

Schrama, E., Scharroo, R., and Naeije, M. (2000). Rads altimeter database system (rads): Toward generic multi-satellite altimeter database system.

Appendices

A Potential errors

A.1 Cycles 287, 007 and 006

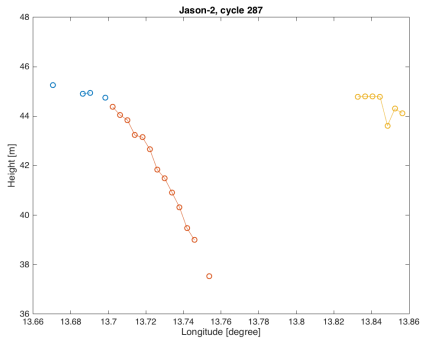

(a) An example of height errors occuring across Vänernj2c287

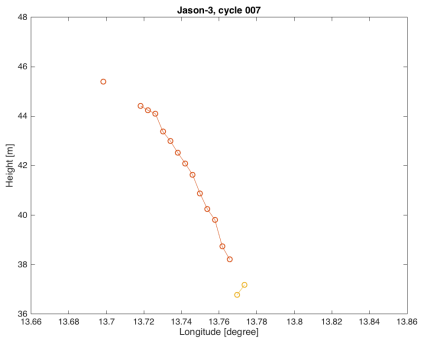

(b) An example of height errors occuring across Vänern: j3c007

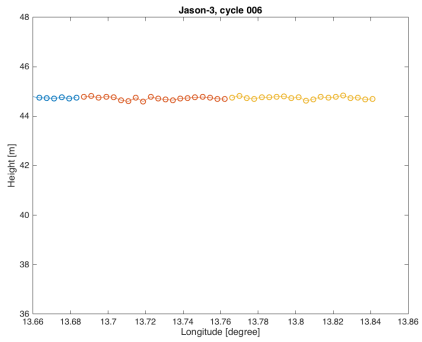

(c) An ideal example of heights across Vänern: c006

Figure 11: Height observations vs. longitude, illustrating the errors signaled for cycles 287/007. Cycle 006 is just to a good example.

B Matlab scripts

B.1 jason21.m

```
1 clear all; close all; clc;
2
3 % load data
```

```
4  d=nc_reader('JASON3/JA3_IPN_2PTP007_220_20160425_113058_20160425_122711.nc'); % jason3
5  j=nc_reader('JASON2/JA2_IPN_2PdP287_220_20160425_112934_20160425_122547.nc'); % jason2
6
7  % area
8  sverige20hz=find(d.lat_20hz>58.9 & d.lat_20hz<59.2 & d.lon_20hz > 13.5 & d.lon_20hz < ...
       13.9); % TRACK 220
9  sverige20hzj=find(j.lat_20hz>58.9 & j.lat_20hz<59.2 & j.lon_20hz > 13.5 & j.lon_20hz < ...
       13.9); % TRACK 220
10
11 % lat/lon
12 lat = d.lat_20hz(sverige20hz);
13 lon = d.lon_20hz(sverige20hz);
14
15 latj = j.lat_20hz(sverige20hzj);
16 lonj = j.lon_20hz(sverige20hzj);
17
18 %mean positions
19 disp('position J3')
20 [mean(lat) mean(lon)]
21
22 disp('position J2')
23 [mean(latj) mean(lonj)]
24
25 %global plot showing track 220
26 figure(1)
27 scatter(d.lon_20hz(:),d.lat_20hz(:),10,'filled');
28 hold on
29 S = shaperead('landareas','UseGeoCoords',true);
30 geoshow([S.Lat], [S.Lon],'Color','black');
31 axis([-180 180 -90 90])
32 xlabel('Longitude [degree]');
33 ylabel('Latitude [degree]');
34 plot_google_map
35
36 % plot showing seleceted data ¬73-75 points
37 figure(2)
38 scatter(d.lon_20hz(sverige20hz),d.lat_20hz(sverige20hz),10,'filled');
39 hold on
40 S = shaperead('landareas','UseGeoCoords',true);
41 geoshow([S.Lat], [S.Lon],'Color','black');
42 axis([0 30 50 60])
43 xlabel('Longitude [degree]');
44 ylabel('Latitude [degree]');
45 plot_google_map
```

```
46
47 % Altitude, range and corrections
48 alt = d.alt_20hz(:);
49 altj = j.alt_20hz(:);
50
51 range = d.range_20hz_ku(:);
52 rangej = j.range_20hz_ku(:);
53
54 %wet = interp(d.model_wet_tropo_corr,20);
55 wet = interp(d.rad_wet_tropo_corr,20);
56 dry = interp(d.model_dry_tropo_corr,20);
57 iono = interp(d.iono_corr_gim_ku,20);
58
59 wetj = interp(j.rad_wet_tropo_corr,20);
60 dryj = interp(j.model_dry_tropo_corr,20);
61 ionoj = interp(j.iono_corr_gim_ku,20);
62
63 % ssb = interp(d.sea_state_bias_ku,20);
64 % inv = interp(d.inv_bar_corr,20);
65 % invj = interp(j.inv_bar_corr,20);
66
67 pole = interp(d.pole_tide,20);
68 load = interp(d.load_tide_sol1,20);
69 solid = interp(d.solid_earth_tide,20);
70 geoid = interp(d.geoid,20);
71
72 polej = interp(j.pole_tide,20);
73 loadj = interp(j.load_tide_sol1,20);
74 solidj = interp(j.solid_earth_tide,20);
75 geoidj = interp(j.geoid,20);
76
77 %% mean values and standard deviation for jason3
78 disp('jason3');
79
80 range_corr = range+wet+dry+iono;
81
82 water_level = alt-range_corr;
83
84 water_geoid = water_level-pole-load-solid-geoid;
85
86 water = water_geoid;
87
88 % condition
89 water(abs(water - nanmean(water)) > abs(3*nanstd(water)))=nan;
```

```
water(abs(water - nanmean(water)) > abs(3*nanstd(water)))=nan;
water(abs(water - nanmean(water)) > abs(3*nanstd(water)))=nan;

nanmean(water)
nanstd(water)

%% mean values and standard deviation for jason3
disp('jason2');

range_corrj = rangej+wetj+dryj+ionoj;

water_levelj = altj-range_corrj;

water_geoidj = water_levelj-polej-loadj-solidj-geoidj;

waterj = water_geoidj;

% condition
waterj(abs(waterj - nanmean(waterj)) > abs(3*nanstd(waterj)))=nan;
waterj(abs(waterj - nanmean(waterj)) > abs(3*nanstd(waterj)))=nan;
waterj(abs(waterj - nanmean(waterj)) > abs(3*nanstd(waterj)))=nan;

nanmean(waterj)
nanstd(waterj)

% American style (20 x 3)

K = reshape(water(3:62),[20,3]);
L = reshape(waterj(8:67),[20,3]);
```

B.2 soe vs sat.m

```
clear all; close all; clc;

% Vanern data from 1938-now
fid = fopen('wasserdu.txt'); % hent ny vnern
a = textscan(fid, '%s  %f  %s');
fclose(fid);
height=a{2};
time=a{1};

vand = height(28536:1:28615)./100+0.69;
```

```
% +0.69 is due to the adjustment to achieve same level of reference

% jasontre = [44.7970 44.7547 44.7176 NaN 44.7069 44.7132 44.7327 42.8069];
% jasonto = [44.8035 44.7846 44.7364 39.9695 44.7366 NaN 44.7616 44.8167];

% mean of section of 20 observations (20 x 3)
Jason3 = [  44.7939   44.7734   44.8019;    %date 02.16
            44.7426   44.7402   44.7668;    %02.25
            44.6976   44.7344   44.7140;      %03.06
            NaN, NaN, NaN;                  %03.16
            44.7005   44.7107   44.7031;      %03.26
            44.7480   44.7061   44.7036;      %04.05
            44.7275   44.7221   44.7484;      %04.15
            NaN   42.0483   36.9833;            %04.25
            44.7991 44.8031  44.7899];        %05.05
%            44.7399   44.7459   44.7707];         %05.15

Jason2 = [44.8190   44.7715   44.8198;    %02.16
          44.7706   44.7777   44.7848;    %02.25
          44.7364  44.7425   44.7315;    %03.06
          36.8327, NaN, NaN;                %03.16
          44.7447   44.7305   44.7316;     %03.26
          NaN, NaN, NaN;                %04.05
          44.7564   44.7760   44.7504;    %04.15
          44.9667   41.6834   44.4603  ;%04.25
          44.7974   44.8389   44.8173]; %05.05
%           44.7457   44.7509   44.7996];   %05.15


t = datetime(time); % rewriting 'time'

figure(2)
set(gca,'YTick', 44.5:0.05:45.5); % plotter sat hver 10ende dag og vand hver dag...
plot(t(28536:1:28615),vand','d','MarkerFaceColor',[0 0 1]);
hold on; plot(t([28536,28545,28555:10:28615]),Jason2,'+','MarkerEdgeColor',[0 .7 ...
    .7],'MarkerFaceColor',[0 0.7 0.7]);
plot(t([28536,28545,28555:10:28615]),Jason3,'o','MarkerEdgeColor','red','MarkerFaceColor','red');
%title('Water level height','fontsize',16)
xlabel('Date [days]','fontsize',16)
ylabel('Height [m]','fontsize',16)
ylim([44.4 45.4])
grid on
grid minor
%legend('water station','Jason-2','Jason-3')
```

```
54
55 % disp('std: mean - vand')
56 % nanstd(jasontre'-wasser)
57 % nanstd(jasonto'-wasser)
58 % disp('std hver tyvende')
59 % nanstd(Jason3(:))
60 % nanstd(Jason2(:))
61 %
62 % disp('rms hver tyvende')
63 % rms(Jason3(isnan(Jason3)==0))
64 % rms(Jason2(isnan(Jason2)==0))
```

B.3 function: world.m

```
1  function [gridsla, gridswh, mlat, ngrid] = world(lat,sla, swh,res)
2
3  mlat = floor(min(lat):res:max(lat));
4  %mlon = floor(min(lon):max(lon));
5
6  %latgrid = zeros(length(mlat),1)*NaN;
7  %longrid = zeros(length(mlat),length(mlon))*NaN;
8  gridsla = zeros(length(mlat),1)*NaN;
9  gridswh = zeros(length(mlat),1)*NaN;
10 ngrid = zeros(length(mlat),1)*NaN;
11
12 for ii = 1:length(mlat)-1;
13     mask =  (mlat(ii)≤ lat) & (mlat(ii+1)≥lat); % starter fra lat:-67 op til lat:65
14     obssla = sla(mask);
15     obsswh = swh(mask);
16     ngrid(ii,1) = length(obssla);
17     gridsla(ii,1) = rms(obssla);
18     gridswh(ii,1) = rms(obsswh);
19
20 end
21
22 gridsla = smooth(gridsla,0.09,'loess');
23 gridswh = smooth(gridswh, 0.09,'loess');
```

B.4 xo.m

```
%% xovers
clc; close all; clc;

xo = load('cyclefour.rxf'); %load cycle
load coastlines
J2 = (1:6773); % single
J3 = (6774:14187); % single
%dual = (xo(14188:end));

res = 1
lat = xo(J2,1);
lon = xo(J2,2);
sla = xo(J2,3);
%SWH = xo(J2,5);

figure(1) % global scatter plot af single J2
scatter(lon,lat,30,sla,'filled'); hold on; plot(coastlon, coastlat);
%title( 'J2-J2 [m]','fontsize',16);
xlabel('Latitude [deg]','fontsize',16)
ylabel('Longitude [deg]','fontsize',16)
colormap(jet)
c=colorbar; title(c,'[m]')
caxis([-0.05 0.05])
hold off;


lat = xo(J3,1);
lon = xo(J3,2);
sla = xo(J3,3);


figure(2) % global scatter plot of single J3
scatter(lon,lat,30,sla,'filled');hold on;
plot(coastlon, coastlat);
%title( 'J3-J3 [m]','fontsize',16);
xlabel('Latitude [deg]','fontsize',16);
ylabel('Longitude [deg]','fontsize',16);
colormap(jet)
c=colorbar;title(c,'[m]');
caxis([-0.1 0.1]);
hold off;


figure(4) % global scatter plot of dual J2-J3
```

```
scatter(xo(14188:end,2),xo(14188:end,1),30,xo(14188:end,3),'filled');hold on;
plot(coastlon, coastlat);
%title( 'J2-J3 [m]','fontsize',16);
xlabel('Latitude [deg]','fontsize',16)
ylabel('Longitude [deg]','fontsize',16)
colormap(jet)
c=colorbar; title(c,'[m]');
caxis([-0.1 0.1]);
hold off;

%%
```

B.5 anomaly.m

```
% crossover profiles

xo = load('dual4.rxf');
J2 = (1:6773);
J3 = (6774:14187);

res = 1;

lat = xo(J2,1);
lon = xo(J2,2);
sla = xo(J2,3);
swh = xo(J2,5);

[gridsla, gridswh, mlat, ngrid] = world(lat,sla, swh,res);

figure(1)
subplot(1,2,1)
plot(gridsla(isnan(gridsla)==0),mlat(isnan(gridsla)==0)); hold on;
%xlim([0 2])
xlim([-0.15 0.15])
%xlim([-0.04 0.04])

lat = xo(J3,1);
lon = xo(J3,2);
sla = xo(J3,3);
swh = xo(J3,5);

[gridsla, gridswh, mlat, ngrid] = world(lat,sla, swh,res);
```

```
29
30 plot(gridsla(isnan(gridsla)==0),mlat(isnan(gridsla)==0));
31 legend('J2-J2','J3-J3')
32 xlabel('SLA [m]','fontsize',16)
33 ylabel('Latitude [deg]','fontsize',16)
34 grid
35 %xlim([0 2])
36 xlim([-0.15 0.15])
37 %xlim([-0.04 0.04]);
38 hold off;
39 title('Single satellite')
40
41 %%
42
43 lat = xo(14188:end,1);
44 lon = xo(14188:end,2);
45 sla = xo(14188:end,3);
46 swh = xo(14188:end,5);
47
48 [gridsla, gridswh, mlat, ngrid] = world(lat,sla, swh,res);
49
50 subplot(1,2,2)
51 plot(gridsla(isnan(gridsla)==0),mlat(isnan(gridsla)==0));
52 legend('J2-J3')
53 xlabel('SLA [m]','fontsize',16)
54 ylabel('Latitude [deg]','fontsize',16)
55 %xlim([0 2])
56 xlim([-0.15 0.15])
57 %xlim([0.0 0.08])
58 grid
59 hold off;
60 title('Dual satellite')
61
62 % figure(2)
63 % plot(gridswh(isnan(gridsla)==0),mlat(isnan(gridsla)==0));
64 % legend('J2-J3')
65 % xlabel('SWH [m]','fontsize',16)
66 % ylabel('Latitude [deg]','fontsize',16)
67 % xlim([-0.15 0.15])
68 % hold off;
69 % title('Significant Wave Height')
70 %
71 % figure(3)
72 % plot(gridswh,gridsla,'*')
```

```
% plot(abs(gridswh),gridsla,'*')
% xlabel('SWH [m]','fontsize',16)
% ylabel('SLA [m]','fontsize',16)
% axis([0 0.15 0.04 0.07])
% %title('Linear fit')
```